SIMULTANEOUS ORIENTATION OF BRIGHTNESS, RANGE AND INTENSITY IMAGES

A. Wendt[a,b], C. Heipke[b]

[a]Institute for Applied Photogrammetry and Geoinformatics, University of Applied Sciences Oldenburg,
Ofener Str. 16/19, 26121 Oldenburg, Germany
[b]Institute of Photogrammetry and GeoInformation, University of Hannover,
Nienburger Str. 1, 30167 Hannover, Germany - wendt@ipi.uni-hannover.de

Commission V, WG V/3

KEY WORDS: Orientation, Surface matching, Reconstruction, Data fusion, Terrestrial laser scanning

ABSTRACT:

Within the scope of a common evaluation of brightness, range and intensity images, this article introduces a new area based approach to achieve the simultaneous orientation of multiple data types. The actual innovation is the combined least-squares adjustment, which is an extension of object space image matching with ranges and intensities as additional observations. The complete mathematical model is specified and discussed. For a representation of complex object surfaces, the simultaneous consideration of multiple surface patches is described. The principle of this approach is shown with a synthetic data sample and evaluated with a real data set of a hybrid terrestrial laser scanner. In the experiments it is demonstrated, that in cases where the orientation of single sensors fails, the simultaneous orientation of hybrid sensors is still successful. Additionally, it is shown that the simultaneous surface reconstruction improves the orientation results and that brightness images can be oriented relative to laser scanner data including range and intensity images.

1 INTRODUCTION

1.1 Motivation

Documentation of building facades is useful in a variety of applications such as architecture, cultural heritage recording, virtual reality and urban planning. Currently, the standard technique for data capture is terrestrial photogrammetry. In recent times terrestrial laser scanning has gained importance. Also hybrid systems have been developed, which delivers range and intensity images from the laser scanner and brightness images from the camera. In general, the relative orientation between the two sensors of a hybrid system is pre-calibrated and thus known with 3 translations and 3 rotations.

These optical measurement techniques provide brightness images, range images and intensity images of the facade. Brightness images deliver the texture and range images directly the geometric information of the viewed object scene, see fig. 1. The intensity images are additionally obtained from the laser scanner and contain the energy of the emitted laser signal, which is reflected back in the direction of the sensor. Due to their different potential these data types complement each other and also include redundant information. For instance, the brightness images give visual information of the object scene and also indirect geometric information, i.e. through stereoscopy and image matching. Image matching is an ill-posed problem and needs good approximate values of the surface parameter, which can be provided by a laser scanner. This is only one example that shows that the fusion of both data types significantly increases the potential of optical measurement techniques.

Figure 1: The potential of different image types. From left to right: Brightness, range and intensity image.

However, the orientation of the images is a prerequisite for any photogrammetric task involving the transformation between the different sensor data. A new image based approach for the simultaneous orientation of multiple sensors is presented in this paper. Preliminary

work on this approach can be found in Wendt & Heipke (2005).

1.2 Related work

For the area-based orientation of images taken from different positions, also known as registration, several approaches have been developed in photogrammetry and computer vision.

A general overview of the orientation of brightness images is given by Heipke (1997). In the context of this paper only object based image matching algorithms are relevant. These algorithms are published in detail in literature, e.g. Ebner et al. (1987), Wrobel (1987) and Helava (1988). The functional model includes the sensor parameters, the image orientation and the parameter of the surface function. Kempa (1995) demonstrates the estimation of the image orientation beside the surface reconstruction. Strunz (1993) and Rosenholm & Torlegard (1988) show how to orient aerial images with surfaces in object space. These remarks on brightness image orientation are also relevant for intensity images.

For range images the task is usually accomplished by formulating the problem as an optimization: a cost function is set up, based on metrically estimating the distance between the corresponding entities of a surface measured in different views. The optimization techniques differ by the formulation of the entities as well as the minimization techniques. The essential difficulty of orientation is the identification of entities in different images corresponding to the same surface. To solve this task a lot of research has been carried out in feature extraction, feature description and matching algorithms. The goal is to find view point invariant matching features, to describe them as unique as possible, also with additional attributes added to the range elements, and to recognize correspondences in the overlapping data sets. For the recognition a large variety of optimization methods has also been developed.

For an general overview concerning range data orientation refer e.g. to Grün & Akca (2004), Rusinkiewicz & Levoy (2001) and Williams et al. (1999).

Several approaches have been presented based on the principle of the Iterative Closest Point (ICP) algorithm introduced by Besl & McKay (1992), Chen & Medioni (1992) and Zhang (1994). The algorithm directly works with point clouds in object space and assumes that one point set is a subset of the other. The basic idea of the ICP algorithm is that the closest points approximate the true point correspondences. Modifications of this algorithm were developed for multiple point cloud orientation and for increasing the accuracy and reliability of the results, e.g. by giving each point of the cloud additional attributes, like texture (Johnson & Kang, 1997). Godin et al. (2001) give each range image element invariant attributes and use the Iterative Closest Compatible Point (ICCP) algorithm for the registration process, where a point is compatible if the value of some associated invariant feature, like surface curvature, intensity measurements or color, is within a given threshold. The ICCP minimizes distances between a point and the corresponding tangential plane of its corresponding candidate. Weik (1997) exploits intensity and gradient information to determine corresponding point sets on the partial surfaces using an optical flow approach. Pulli (1997) obtained corresponding candidates by projecting complete colored meshes against others, performing 2D image alignment, and pairing mesh points ending at the same pixel. Gelfand et al. (2005) develop a global registration algorithm, based on robust feature identification and correspondence search using geometric descriptors. Litke et al. (2005) introduce an image processing approach for surface matching, where instead of matching two surfaces directly in 3D, a well-established matching methods from image processing in the parameter domains of the surfaces was applied.

A further extension of the ICP algorithm with regard to the surface description is given by Grün & Akca (2004). There, the point cloud is represented as a patch-wise surface function. Akca (2005) introduces an extension of this surface matching approach by using additional intensity values and other surface based data. Kraus et al. (2006) modify the least-squares matching for strip adjustment and quality control for airborne laser scanner data. They introduce a template matching approach, using height, intensity and slope information. Neugebauer (1997) shows how to directly use range images to solve the orientation problem. The surface is implicitly specified in the range image as a function of the observed ranges.

One weakness of the approaches of range and brightness orientation is the limited use of multi-source data. Additional data is mostly treated as an attribute of the master data source. In this research we deal with data sets of objects recorded with more than one sensor type and multiple views simultaneously. The goal is to use the full potential of the recorded data for the orientation estimation.

2 THE NEW ORIENTATION CONCEPT

In this section a new approach for the simultaneous orientation of multiple images is introduced. It is a general approach to orient images of multiple sensors with and without known relative orientation. The orientation concept is based on the combination of object based image

matching and the exploitation of range and intensity images. The innovation is that image rays of brightness, intensities and ranges are combined in a least-squares adjustment.

2.1 The functional model

For the model description, the definition of the various coordinate systems, the orientation of the individual sensors in object space, the transformation between sensor space and object space and the definition of the object surface must be introduced, see fig. 2.

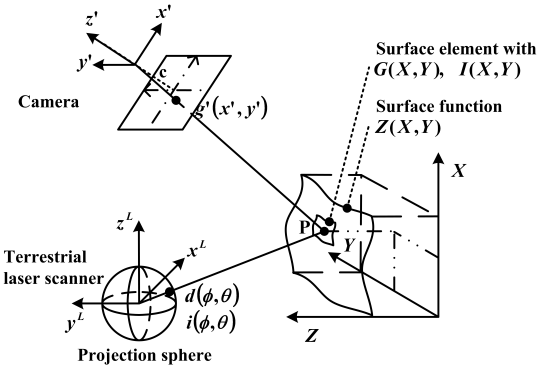

Figure 2: Parameters of the functional model

In sensor space of the brightness image, the coordinate system [x',y',z'] is defined with the origin at the projection center. Concerning the range image, the sensor system origin $[x^L, y^L, z^L]$ is defined as the center of the terrestrial laser scanner. In both sensor systems, the x- and y-axis are defined in the row and column direction of the image. The intensity image is related to the same sensor system as the range image. The object surface $Z(X,Y)$ is given in the object space coordinate system [X,Y,Z], e.g. in a grid, defined by 4 node points for each grid cell and an interpolation function, e.g. bilinear. Within each grid cell a predefined number of surface elements for the brightness values $G(X,Y)$ and the intensity values $I(X,Y)$ is defined, see fig. 2. The exterior orientation of the sensor referring to the object space is given by $O^C(\mathbf{T}^C, \mathbf{R}^C)$ for the brightness image and $O^L(\mathbf{T}^L, \mathbf{R}^L)$ for the laser data. The parameters of the orientation consist of three translations $\mathbf{T}(t_X, t_Y, t_Z)$ and three rotations around the X,Y and Z axis, respectively, captured in the rotation matrix $\mathbf{R}(r_{11}, r_{12}, \cdots, r_{33})$. The relation of a brightness value $g'(x', y')$ to the corresponding grey value $G(X,Y)$ of a surface element (X,Y) in object space is outlined in fig. 2. The brightness is a function of the image coordinates, which in turn depend on the object coordinates and the image orientation through the collinearity eqs.

$$g'(x', y') = G(X,Y) \tag{1}$$

with

$$x' = -c\frac{r^C_{11}\Delta X + r^C_{21}\Delta Y + r^C_{31}\Delta Z}{r^C_{13}\Delta X + r^C_{23}\Delta Y + r^C_{33}\Delta Z} \tag{2}$$

and

$$y' = -c\frac{r^C_{12}\Delta X + r^C_{22}\Delta Y + r^C_{32}\Delta Z}{r^C_{13}\Delta X + r^C_{23}\Delta Y + r^C_{33}\Delta Z} \tag{3}$$

with

$$\Delta X = X - t^C_x, \Delta Y = Y - t^C_y, \Delta Z = Z(X,Y) - t^C_z.$$

The range values of the laser scanner are expressed as distances d in a direction (ϕ, θ) relative to the $[x^L, y^L, z^L]$ system. ϕ is the angle between the x^L-axis and the direction of d projected into the $x^L y^L$ plane and θ the angle between the direction of d and z^L-axis. The observed range d is identical to the distance s between the observed surface point and the origin of the laser scanner:

$$d(\phi, \theta) = s \tag{4}$$

with

$$\phi = \arctan(\frac{y^L}{x^L}) \tag{5}$$

and

$$\theta = \arctan(\frac{\sqrt{(x^L)^2 + (y^L)^2}}{z^L}) \tag{6}$$

and

$$s = \sqrt{(X - t^L_X)^2 + (Y - t^L_Y)^2 + (Z(X,Y) - t^L_Z)^2} \tag{7}$$

For the relation of a range value d to the surface function in object space, the transformation between the range image sensor system and the object space system is necessary:

$$\begin{pmatrix} x^L \\ y^L \\ z^L \end{pmatrix} = \begin{pmatrix} \mathbf{R^L} \end{pmatrix}^T \begin{pmatrix} X - t^L_X \\ Y - t^L_Y \\ Z(X,Y) - t^L_Z \end{pmatrix} \tag{8}$$

The intensity value i is also a function of its image coordinates which depend on the object coordinates and the image orientation through the collinearity eqs. The relation of a intensity value $i(\phi, \theta)$ to the corresponding reflectance value $I(X,Y)$ of a surface element (X,Y) in object space is:

$$i(\phi, \theta) = I(X,Y) \tag{9}$$

In this case the intensity value i is a function of the same image coordinates as the range value. Thus, eqs. (5), (6) and (8) are also relevant for the functional description of (9).

2.2 Sensor specific extensions

In the case of hybrid sensors the relative orientation between the camera and the laser scanner coordinate system is given by:

$$\mathbf{e} = \mathbf{T}^C - \mathbf{T}^L \tag{10}$$

and

$$\mathbf{R}_C^L = \mathbf{R}^L(\mathbf{R}^C)^{-1} = \mathbf{R}^L(\mathbf{R}^C)^T \tag{11}$$

with $\mathbf{e}$ the eccentricity vector between the perspective centers of the camera and laser scanner and $\mathbf{R}_C^L$ the rotation matrix between the two coordinate systems. For hybrid sensors, $\mathbf{e}$ and $\mathbf{R}_C^L$ may be known from a calibration step.

The brightness values in image space vary depending on the light source, surface reflectance and further parameters. Therefore, a light and reflection model has to be included to adjust eq. (1). In the case of small parts on the surface a linear transfer function between the brightness value g' and the grey value G in object space is assumed to be sufficient. Eq. (1) then reads:

$$t_0 + t_1(g'(x', y')) = G(X, Y) \tag{12}$$

with linear transfer parameters for offset t_0 and scale factor t_1.

Finally, a normalization of the intensity values using the squared distance d should be introduced, since the amount of energy received at a certain surface patch is indirectly proportional to the squared distance:

$$\frac{i(\phi, \theta)}{d^2} = I(X, Y) \tag{13}$$

2.3 Simultaneous consideration of multiple surface patches

So far, the surface in object space has been described with one surface patch, cf. fig. 2. In the case of large or complex 3D objects this description is not sufficient. In this new orientation approach multiple surface patches are introduced, as is shown in fig. 3.

Each patch represents a part of the surface with a separate surface function described in a local coordinate system $[X^{S_i}, Y^{S_i}, Z^{S_i}]$; with $i = 1, \ldots n$. These patches are located in areas of geometric surface variation or good brightness texture. The size of each patch can be chosen individually. Unless given otherwise, the object coordinate system $[X, Y, Z]$ is defined in the first patch, and the orientations of the other patches with respect to the first are described by the values $\mathbf{O}^{S_i}(\ \mathbf{T}^{S_i}, \mathbf{R}^{S_i})$. For instance, the transformation of the point $\mathbf{V}^{S_n}$ of the

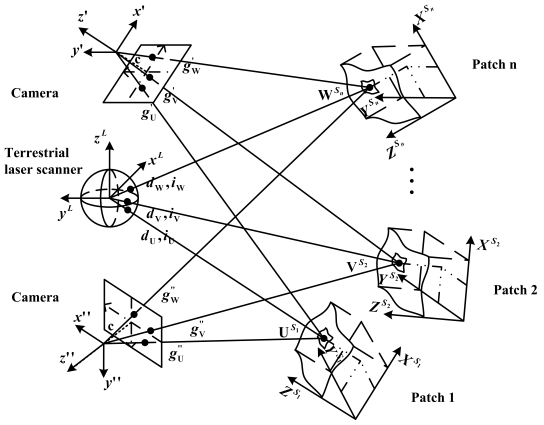

Figure 3: Simultaneous use of multiple surface patches

n^{th} surface patch coordinate system $[X^{S_n}, Y^{S_n}, Z^{S_n}]$ into the object space coordinate system is:

$$\begin{pmatrix} X_V \\ Y_V \\ Z_V \end{pmatrix} = \mathbf{T}^{S_n} + \mathbf{R}^{S_n} \begin{pmatrix} X_V^{S_n} \\ Y_V^{S_n} \\ Z_V^{S_n} \end{pmatrix} \tag{14}$$

2.4 Adjustment approach

In the following, the image orientations O, the surface function $Z(X, Y)$ as well as the grey values $G(X, Y)$ and reflectance values $I(X, Y)$ of the surface elements, are considered as unknowns. The resulting non-linear observation eqs. read:

$$v_C = \widehat{G}(X, Y) - (t_0 + t_1(g'(x'(\widehat{O}^C, \widehat{Z}(X, Y)), y'(\widehat{O}^C), \widehat{Z}(X, Y)))) \tag{15}$$

and

$$v_L = s(\widehat{O}^L, \widehat{Z}(X, Y)) - d \cdot (\phi\{x^L(\widehat{O}^L, \widehat{Z}(X, Y)), y^L(\widehat{O}^L, \widehat{Z}(X, Y))\}, \theta\{x^L(\widehat{O}^L, \widehat{Z}(X, Y)), y^L(\widehat{O}^L, \widehat{Z}(X, Y)), z^L(\widehat{O}^L, \widehat{Z}(X, Y))\}) \tag{16}$$

and

$$v_I = \widehat{I}(X, Y) - \frac{i}{d^2} \cdot (\phi(x^L(\widehat{O}^L, \widehat{Z}(X, Y)), y^L(\widehat{O}^L, \widehat{Z}(X, Y))), \theta(x^L(\widehat{O}^L, \widehat{Z}(X, Y)), y^L(\widehat{O}^L, \widehat{Z}(X, Y)), z^L(\widehat{O}^L, \widehat{Z}(X, Y)))) \tag{17}$$

with v_C, v_L, v_I being the adjustment residuals. For reasons of simplicity, the eqs. are only given for one surface patch, an extension to multiple patches is straight forward. Eqs. (15), (16) and (17) have to be linearized with respect to the unknowns. The adjustment is then solved iteratively using standard formulae. In the case of known relative orientation of a hybrid sensor data set, the exterior orientation of the brightness images is replaced by the orientations of the laser scanner using eqs. (10) and (11).

3 EXPERIMENTS

Experimental testing was carried out to demonstrate that:

- in cases where the orientation of single sensors fails, the simultaneous orientation of hybrid sensors is still successful
- simultaneous surface reconstruction improves the orientation results
- individual brightness images can be oriented relative to range and intensity images

The experiments have been performed with both synthetic and real data. To solve the non-linear adjustment, initial values have to be provided by manual measurements, standard procedures of terrestrial laser scanner data orientation or alternative orientation techniques. Also the free datum parameters have to be fixed. In our case, the datum is defined by 3 translations and 3 rotations. To define the datum we fix one viewpoint orientation. Alternatively, the datum could be fixed with direct observations of the datum parameters, measurements of signalized points or known surfaces in object space. For the assessment of the test results, the theoretical standard deviation of the unknowns and the root mean square (RMS) values of the different groups of observation in object space are considered.

3.1 Synthetic data

A synthetic data set is used to demonstrate that in cases when the orientation of single sensors fails, the simultaneous orientation of hybrid sensors with known values for $\mathbf{e}$ and $\mathbf{R}_C^L$ (see eq. (10) and (11)) is still successful.

The data set contains two adjacent surface patches and two view points of a hybrid sensor. The images conform to normal case stereo images. The object surface of the first patch contains a geometric strip and the second surface patch a rotated radiometric strip. Each surface patch is described with 21 by 21 geometric grid elements and 300 by 300 brightness grid elements. The

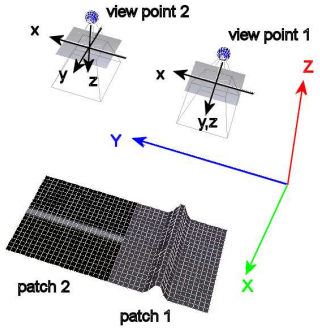

Figure 4: Synthetic data set up

patches cover an area of 20 m by 20 m each and the distance from the patches to the sensor is 50 m. The baseline between the sensors is 20 m. In fig. 4 the set up is shown, the cameras mark the viewpoints of the hybrid sensor. The X-axis is in the viewing direction to the surface patch. The Y- and Z-axis are parallel to the surface patch.

The sensor orientation was computed for the following cases:

1. only brightness images
2. only range images
3. brightness and range images simultaneously

The different observations are all assigned to equal weights. The iterations were terminated after two successive estimates of the unknowns differed by less than one per mille. If the true position of the viewpoint cannot be estimated correctly and accurately, the orientation process is deemed to have failed.

In table 1 a comparison between the theoretical standard deviations of the estimated orientation parameters is listed.

	$s_{\mathbf{T}_x}[m]$	$s_{\mathbf{T}_y}[m]$	$s_{\mathbf{T}_z}[m]$
1	–	∞	–
2	2.8e-003	9.7e-003	6.0e+000
3	2.8e-003	8.5e-003	5.9e-003
	$s_{\mathbf{R}_x}[rad]$	$s_{\mathbf{R}_y}[rad]$	$s_{\mathbf{R}_z}[rad]$
1	–	–	–
2	2.2e-004	1.8e-004	8.7e-005
3	3.4e-006	5.9e-005	8.6e-005

Table 1: Theoretical standard deviations of the orientation parameters of the synthetic data set

In case 1), the radiometric strip runs parallel to the baseline and it is mapped into the central row of the brightness image. The image gradients in that direction become zero, which results in a singular matrix of normal equations. The orientation estimation fails. In case 2), the worst value of the theoretical standard deviation is in the Z-direction along the geometric strip. Due to numerical reasons it does not become infinite. However, the orientation estimation is also wrong. Only in case 3), the orientation process is successful in all directions.

3.2 Real data

With the real data set it is shown that the simultaneous surface reconstruction improves the orientation estimation. The orientation is carried out with view points of a hybrid laser scanner including brightness, range and intensity images. It is also shown that individual brightness images can be oriented relative to laser scanner data within the simultaneous orientation estimation and surface reconstruction.

In the following, three view points of the data set *Dresdner Frauenkirche* are used. The data set was recorded with the hybrid laser scanner Riegl LSM-Z420i. Compared to the synthetic data set, additional effects, like differences in contrast, varying baselines and varying sensor to object distances occur. Additionally, intensity images are available. Calibration values for $\mathbf{e}$ and $\mathbf{R}_C^L$ between the laser scanner were determined through the standard procedure of the sensor manufacturer. Sensor orientation values were also available and were introduced as initial values.

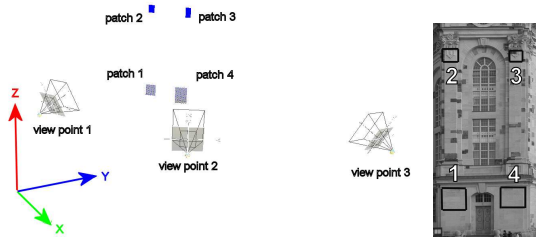

Figure 5: Real data setup. Left: Surface patch distribution in relation to the view points. Right: Chosen surface patches on the facade.

For the orientation test 4 surface patches distributed on the facade were chosen, cf. fig. 5. The patches are modeled with a geometric grid size of 0.06 m and a radiometric grid size of 0.02 m. The resolution of the range and intensity image is about 0.04 m and of the brightness image about 0.03 m in object space. The accuracy for a single range measurement is specified with 0.01 m by the manufacturer. The test, with its planar geometric characteristics represents a typical case in facade modeling. The real data set contains problematic aspects: the range images are a little noisy and the intensity images contain a lot of noise. All images include occlusions, because of the different perspective views. The effects are considered by:

- different weights for the observations
- a stabilizing function including curvature minimizers for the surface reconstruction

The stabilization function is used to bridge information gaps and image noise and is implemented according to Terzopoulos (1988). The function is an additional observation concerning the surface reconstruction. The range observations are used with the weight of 1, the brightness and intensity observations with a weight of 1/1000. The stabilizing function is considered with 1/10. In the following three adjustments are carried out:

1. hybrid sensor orientation, given surface
2. hybrid sensor orientation, surface unknown
3. individual sensor orientation, surface unknown

In case 1), the surface of the patches is given by the range image of the first view point, and is not reconstructed within the adjustment. For the orientation brightness, range and intensity images are used simultaneously. In the case 2), the surface and the orientation parameters of the hybrid sensors are estimated simultaneously. In case 3), the camera is treated as an individual sensor. The brightness images are oriented relative to the laser scanner data and are also used to reconstruct the surface.

	RMS G [0..255]	RMS s [m]	RMS I [0..1]
1	7.5	0.010	0.026
2	4.6	0.015	0.013
3	3.6	0.016	0.013

Table 2: RMS values in object space of the real data adjustment.

All calculations were successful, in table 2 the resulting root mean square (RMS) values of the observations in object space from the three adjustments are shown. The simultaneous reconstruction of the surface compared to the given surface in case 1) leads to an improvement for the brightness and intensity values. The RMS value of the range image observations decreases, but considering the spatial resolution of 0.04 m it is still within the signal noise. In case 3), a further improvement for the brightness images could be reached.

In fig. 6 a visualization of the resulting surface and ortho images of patch 2 is shown. Similarities between the geometric surface and the brightness ortho images can be found easily. The dark corner of the intensity image corresponds to changing material on the surface as also seen in the brightness image.

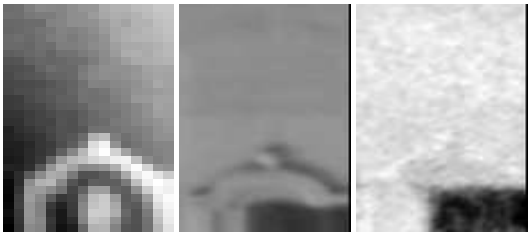

Figure 6: Results for patch 2. From left to right: geometric grid, ortho image of the brightness values, ortho image of intensity values.

4 CONCLUSIONS

In this paper a new framework for the simultaneous orientation of multi source images has been presented. The approach is area based. Within the alignment process the surface is reconstructed patch-wise simultaneously. Each patch has to be covered by at least one data source. But if brightness, range and intensity images are available, they can be used simultaneously.

With the experiment of the synthetic data set, it is demonstrated that in cases of failing single source image orientation, the simultaneous orientation approach is still successful. With the real data set it is shown, that in case of the simultaneous surface reconstruction an improvement of the image orientation could be reached. It is also demonstrated that individual brightness images could be orientated relative to the laser scanning data.

The resulting RMS values of the experiment with the real data set conclude to noisy data of the input images. An inadequate surface grid size, which leads to discrepancies in the functional model, can be excluded, because of the flat geometry of the chosen patch locations. Also the accuracy of 0.01 m for a single range measurement specified by the manufacturer confirms our statement.

In future work, a test data set will be recorded to provide an assessment of the absolute accuracy and the flexibility of this approach. Also more investigations into the distribution of observations and surface patches and the numeric stability in terms of singularities in the normal equations will be performed.

This approach based on approximate values for the orientation parameters. So far no strategy is introduced to provide approximate values. A future research target is to develop an automatic coarse orientation concept based on the simultaneous consideration of brightness, range and intensity data of hybrid laser scanners.

ACKNOWLEDGEMENTS

The authors would like to thank Mr. Nikolaus Studnicka from RIEGL GmbH for providing the data set *Dresdner Frauenkirche*.

References

Akca, D., 2005. Registration of point clouds using range and intensity information. In: A. Grün, L. V. Gool, M. Pateraki and M. Baltsavias (eds), International Workshop on Recording, Modeling and Visualization of Cultural Heritage, Ascona, Switzerland, May 22–27, Taylor & Francis/Balkema, Leiden, pp. 115–126.

Besl, P. and McKay, N., 1992. A method for registration of 3-d shapes. IEEE Transactions on Pattern Analysis Machine Intelligence 14(2), pp. 239–256.

Chen, Y. and Medioni, G., 1992. Object modeling by registration of laser scanner data. Image and Vision Computing 10(3), pp. 145–155.

Ebner, H., Fritsch, D., Gillessen, W. and Heipke, C., 1987. Integration von bildzuordnung und objektrekonstruktion innerhalb der digitalen photogrammetrie. BuL 55(5), pp. 194–203.

Gelfand, N., Mitra, N. J., Guibas, L. J. and Pottmann, H., 2005. Robust global registration. In: M. Desbrun and H. Pottmann (eds), Eurographics Symposium on Geometry Processing (2005), pp. 197–206.

Godin, G., Laurendau, D. and Bergevin, R., 2001. A method for the registration of attributed range images. Int. Conf. on 3D Imaging and Modeling, Quebec, pp. 179–186.

Grün, A. and Akca, D., 2004. Least squares 3D surface matching. IAPRS, 34(5/W16), (on CD-ROM).

Heipke, C., 1997. Automation of interior, relative, and absolute orientation. ISPRS Journal of Photogrammetry & Remote Sensing 52, pp. 1–19.

Helava, U. V., 1988. Object-space least-squares correlation. Photogrammetric Engineering & Remote Sensing 54(6), pp. 711–714.

Johnson, A. and Kang, S., 1997. Registration and Integration of Textured 3-D Data. In: International Conference on Recent Advances in 3-D Digital Imaging and Modeling, pp. 234–241.

Kempa, M., 1995. Hochaufgelöste Oberflächenbestimmung von Natursteinen und Orientierung von Bildern mit dem Facetten-Stereosehen. Dissertation, Technische Hochschule Darmstadt, Darmstadt.

Kraus, K., Ressl, C. and Roncat, A., 2006. Least squares matching for airborne laser scanner data. 'Fifth International Symposium Turkish-German Joint Geodetic Days 'Geodesy and Geoinformation in the Service of our Daily Life", L. Gründig, O. Altan (ed.), ISBN 3-9809030-4-4, p. 7.

Litke, N., Droske, M., Rumpf, M. and Schröder, P., 2005. An image processing approach to surface matching. In: M. Desbrun and H. Pottmann (eds), Eurographics Symposium on Geometry Processing (2005), pp. 1–10.

Neugebauer, P., 1997. Reconstruction of real-world objects via simultaneous registration and robust combination of multiple range images. International Journal of Shape Modeling 3(1&2), pp. 71–90.

Pulli, K., 1997. Surface Reconstruction and Display from Range and Color Data. PhD thesis, University of Washington, Washington.

Rosenholm, D. and Torlegard, K., 1988. Three-dimensional absolute orientation of stereo models using digital elevation models. Photogrammetric Engineering & Remote Sensing 54(10), pp. 1385–1389.

Rusinkiewicz, S. and Levoy, M., 2001. Efficient variants of the ICP algorithm. Int. Conf. on 3D Digital Imaging and Modeling, Quebec, pp. 145 – 152.

Strunz, G., 1993. Bildorientierung und Objektrekonstruktion mit Punkten, Linien und Flächen. Dissertation, Deutsche Geodätische Kommission, Reihe C, Heft Nr. 408, München.

Terzopoulos, D., 1988. The computation of visible-surface representations. IEEE Transactions on Pattern Analysis Machine Intelligence 10(4), pp. 417–438.

Weik, S., 1997. Registration of 3-D partial surface models using luminance and depth information. In: NRC '97: Proceedings of the International Conference on Recent Advances in 3-D Digital Imaging and Modeling, IEEE Computer Society, Washington, DC, USA, pp. 93–100.

Wendt, A. and Heipke, C., 2005. A concept for the simultaneous orientation of brightness and range images. In: A. Grün, L. V. Gool, M. Pateraki and M. Baltsavias (eds), International Workshop on Recording, Modeling and Visualization of Cultural Heritage, Ascona, Switzerland, May 22–27, Taylor & Francis/Balkema, Leiden, pp. 451–457.

Williams, J., Bennamoun, M. and Latham, S., 1999. Multiple view 3D registration: A review and a new technique. IEEE Int. Conf. on Systems, Man, and Cybernetics, Tokyo, pp. 497–502.

Wrobel, B., 1987. Facets stereo vision (fast vision) - a new approach to computer stereo vision and to digital photogrammetry. In: Fast Processing of Photogrammetric Data. ISPRS Intercommision conference, pp. 231–258.

Zhang, Z., 1994. Iterative point matching for registration of free-form curves and surfaces. International Journal of Computer Vision 13(2), pp. 119–152.